

Parallel Plate Testing and Simulation of Corrugated Plastic Pipe

M^cGrath, T.J., Schafer, B.W.

T.J. M^cGrath, Ph.D., P.E., Principal, tjmcgrath@sgh.com
Simpson Gumpertz & Heger Inc., 297 Broadway, Arlington, MA 02474
tel. (781)643-2000, fax (781)643-2009

B.W. Schafer, Ph.D., Assistant Professor, schafer@jhu.edu
Johns Hopkins University, 203 Latrobe Hall, Baltimore, MD 21218
tel. (410)516-7801, fax (410)516-7473

Submitted July 2002 to:
Committee A2C06 for presentation at the 2003 Transportation Research Board Annual Meeting

Word Count: **Abstract** → 162 **Paper** 3751 + 12 **figures** *250, + 2 **table** *250 = 7251

ABSTRACT

This work presents the results of a series of parallel plate tests and finite element simulations those tests conducted on corrugated HDPE plastic pipe to investigate the role of material and geometry on the behavior of the pipe during the test. Specifically, the work considers parallel plate tests on 1500 mm (60 in.) diameter pipe, and finite element simulation of 450 mm, 750 mm, and 1500 mm (18 in., 30 in. and 60 in.) diameter pipe. It is demonstrated that the applied strain demands in a parallel plate test are largely independent of the loading rate in the test, although the stiffness at 5% deflection and the peak load are strongly rate dependent. The tests and analyses show that the deflection at peak load in the parallel plate test is imperfection sensitive. Further, investigation of strain demands around the profile indicates that the pipe material must carry local strains in excess of those typically assumed to occur in the parallel plate test.

INTRODUCTION

The parallel plate test (ASTM D 2412) is a standardized test for insuring that the bending stiffness and strength of thermoplastic pipe meets specified levels of performance. AASHTO M294 uses the test to assure that corrugated HDPE pipe has required minimum pipe stiffness at 5% deflection (i.e. 5% reduction in diameter), and no buckling or loss of load before 20% deflection. The 5% stiffness criterion relates to handling and installation while the 20% deflection criterion provides necessary ultimate capacity. A series of tests and simulations are presented herein which focus primarily on the modeling and behavior related to the 20% deflection criterion for corrugated plastic pipe. Finite element simulation of solid wall HDPE pipe in the parallel plate test has previously been conducted by others (1). The investigation presented here focuses exclusively on profile wall (corrugated) HDPE pipe. The work begins with basic material behavior, followed by testing and simulation of 1500 mm (60 in.) diameter pipe. Using the findings from the 1500 mm (60 in.) diameter pipe study, further finite element simulations on smaller diameter HDPE pipe are used to demonstrate the role of elastic modulus, imperfection sensitivity, and strain demands. The work concludes with a brief look at hand methods that approximate the local buckling behavior observed in the parallel plate test.

MATERIAL TESTING

Fifteen tensile tests were completed to characterize the material behavior of the HDPE resin used to manufacture the pipe. All stress and strain values are reported as engineering stress and strain.

Constant Displacement Rate Tests

Three tests each were conducted at crosshead rates of 25 mm, 2.5 mm and 0.25 mm/min (1.0 in., 0.1 in., and 0.01 in./min). The results are presented in Figure 1 and Table 1. Examination over the three decades of displacement

rates indicates that as the rate increases the maximum stress increases and the strain at which this stress occurs decreases slightly. The initial modulus, as estimated from strains of 0.5% to 1%, is also given in Table 1. The initial modulus decreases with displacement rate, reflecting the role of “creep” as the time to reach the selected strains increases for the slower displacement rate tests.

Table 1 Constant displacement rate tensile test results

Specimen	Modulus (1)	Peak stress, f_{\max}	Strain at peak stress, $\epsilon_{f\max}$	Test Rate
id	MPa (psi)	MPa (psi)	(%)	mm/min. (in./min)
1	1072.3 (155,630)	26.75 (3883)	9.0	26.7 (1.05)
2	1055.9 (153,250)	26.81 (3891)	9.2	26.7 (1.05)
3	1119.1 (162,420)	26.46 (3,841)	7.2	26.4 (1.04)
ave.	1082.4 (157,100)	26.68 (3,872)	8.5	
4	821.0 (119,160)	21.89 (3,177)	10.9	2.67 (0.105)
5	848.5 (123,150)	22.91 (3,325)	12.1	2.67 (0.105)
6	930.6 (135,060)	22.64 (3,286)	9.4	2.67 (0.105)
ave.	866.7 (125,790)	22.48 (3,263)	10.8	
7	562.4 (81,620)	(2)	(2)	0.249 (0.0098)
8	680.5 (98,770)	18.11 (2,628)	13.2	0.249 (0.0098)
9	596.7 (86,600)	18.13 (2,632)	14.0	0.251 (0.0099)
ave.	613.2 (88,997)	18.12 (2,630)	13.6	

1. Modulus, E, is based on strains from 0.5% to 1%
2. Not tested to peak

Creep

We conducted tensile creep tests at stress levels of 3.11, 7.50, and 13.66 MPa, (451, 1089, and 1982 psi). The results for total strain and creep strain are shown in Figure 2. Examining the creep strain at any fixed time (e.g., $t = 10,000$ seconds) shows that the creep strain is not linear with stress. Nonlinear viscoelastic models are required for modeling such behavior.

Relaxation

We conducted relaxation tests (Figure 3) at strains of 1.1%, 4.3%, and 8.3%. The results indicate that relaxation is nearly linear with the applied stress. As creep exhibited nonlinear behavior with stress this indicates that tensile-creep and tensile-relaxation are not identical material phenomena. The apparent elastic modulus as a function of the initial modulus at 10,000 seconds is given in Figure 3(b).

PARALLEL PLATE TESTS

Parallel plate tests of 1500 mm (60 in.) diameter profile wall HDPE pipe manufactured in 1999, were conducted by the manufacturer, in the presence of the authors at load rates: 50.8 mm/min., 25.4 mm/min. and 12.5 mm/min. (2.0 in./min, 1.0 in./min, 0.5 in./min). The applied load, vertical deflection (crosshead displacement) and horizontal diameter change (measured from valley to valley with a tape measure) was recorded for each test. The results are presented in Figure 5 and Figure 6. The experimental data indicates that:

- stiffness at 5% vertical deflection is rate dependent,
- peak load is rate dependent, but
- change in the horizontal diameter as the vertical deflection increases is rate independent.

The rate independence of the deformations implies rate independence for the strain demands as well. Insofar as failure is controlled by strain demand, deformation at failure is therefore predicted to be largely rate independent. Additional testing on nominally identical 600 mm (24 in.) diameter corrugated plastic pipe specimens also indicates that deformation at failure is largely rate independent (2).

PARALLEL PLATE SIMULATION

The finite element model of the parallel plate test (Figure 4) is a 90° segment (crown-to-springline) of a single corrugation, executed in MSC.NASTRAN (3). Symmetry is enforced at the crown, springline, and valley edges as shown in Figure 4. The model is consistent with the behavior of a corrugation which is independent of any end effects that would exist in an actual test – i.e. the corrugations towards the center of an actual parallel plate test. The contact between the “plate head” and the pipe is modeled as frictionless. The horizontal lines near the crown in Figure 4 are rigid “slidelines”. These rigid elements allow contact along their length and are displaced uniformly towards the pipe at a prescribed rate (e.g., 12.5 mm/min., 0.5 in./min) to simulate the test.

The cross-section geometry is based on average profile dimensions, determined by measuring samples provided by the manufacturer (Figure 4). The profile thickness exhibits slight asymmetry and varies with the depth of the cross-section (thinner at the crest). The HDPE material was modeled as both nonlinear viscoelastic-plastic, and rate independent elastic.

The nonlinear viscoelastic-plastic model was calibrated based on the material testing previously described. For the material model, strain is defined as a summation of the elastic, creep, and plastic strains:

$$\varepsilon(\sigma, t) = \varepsilon_e(\sigma) + \varepsilon_c(\sigma, t) + \varepsilon_p(\sigma)$$

where

ε_e = elastic strain = σ/E , where $E = 157,100$ psi – based on constant displacement rate tests,

ε_c = creep strain = $\varepsilon_c(\sigma, t) = A(\sigma) \left(1 - e^{-R(\sigma)t} \right) + K(\sigma)t$ (ORNL form, see 3)

$A = a\sigma^b$, model c3 $a=7.60 \cdot 10^{-9}$, $b=2$; model c5 $a=10.0 \cdot 10^{-9}$, b =same as c3

$R = c\sigma^d$, model c3 $c=9.62 \cdot 10^{-4}$, $d=0.1$; model c5 c, d same as model c3

$K = e[\sinh(f\sigma)]^g$, model c5 $e=0.56 \cdot 10^{-6}$, $f=8.7 \cdot 10^{-4}$, $g=1.2$; model c5 e, f, g same as model c3

ε_p = plastic (nonrecoverable) strain, defined by (σ, ε_p) in psi and in./in.) pairs:

(0,0), (2000,.0127), (3000,.024) (3400,.037), (3600,.044), (3800,.06), (3900,.08), (3950,.20)

Calibration of the viscoelastic material model (ε_c) is completed using the tensile creep tests along with previously conducted compressive creep tests on HDPE (4). Determination of the ORNL parameters (A, R and K) for a particular test are completed by the following:

- fit the long-term creep strain rate, K , as the best fit slope of the experimental creep strain in the data from $t = 2000$ to $t = 10000$ seconds,
- select a value of $(1/R) = 500$ to provide the bulk of the transition between 50 and 2000 seconds,
- select the primary creep strain, A , so that the creep strain rate is matched at a given time (e.g., 150 seconds).

The selected creep model provides adequate approximation of creep (or creep strain rates) over any single decade of time. The plasticity model (ε_p) is a standard rate independent flow theory plasticity model using von Mises yield criteria and isotropic hardening - the specific bounding curve for σ, ε_p is set equal to the constant displacement rate tests conducted at 25.4 mm/min. (1.0 in./min.).

The behavior of the models is compared to experiments in Figure 5 and Figure 6. The primary areas of nonlinear deformation observed in both the model and the test are:

- inward rolling of the crest near the crown (and invert) at the crest to plate head juncture;
- at larger deformations, local buckling of the crest and sidewall at the crown (and invert);
- local buckling of the liner at the springline; and
- inward (radial) deformation of the crest at the springline.

The primary load carrying mechanism for the pipe is circumferential stress. The crown is in bending with compression in the crest and tension in the valley. The springline is in thrust plus bending with tension in the crest, compression in the valley. The shoulder is largely unstressed. The rolling and local buckling at the crown (crest) results in a shift in the neutral axis as the pipe deflects; at 25% deflection, the neutral axis is lowered (towards the valley) approximately 6 mm (0.25 in.) (in a 91 mm, 3.6 in. deep section) from the elastic neutral axis. Inward radial

movement at the springline has a similar effect on the neutral axis, though in this case the lowering of the neutral axis opposes the raising that occurs due to the thrust.

Observed stress and strain values from the finite element models at 25% deflection are summarized in Table 2. For all models the maximum compressive circumferential strain (compressive strain is negative) occurs in the crest at the crown – both in the middle of the crest and in the corners of the crest. The maximum tensile circumferential strain (tension strain is positive) occurs in the crest of the springline, in the corners. While the maximum strain demands are essentially rate independent, the stress demands are strongly rate dependent. The locations of maximum tensile and compressive stress are not at coincident cross-sections. The maximum compressive stress occurs at the crown crest and is far greater than the tensile stresses at the crown valley, due to the location of the centroidal axis, nearer the valley than the crest. The maximum tensile stress occurs at the springline crest. Compressive stresses at the springline valley are highest at the valley-web-liner juncture, but remain low in the center of the liner. Locations of maximum stress do not necessarily coincide with maximum strain locations (due to creep and relaxation) as stresses tend to be higher particularly at locations of new contact between the pipe and loading platen. Although circumferential stress (and strain) are the primary actions in the pipe, rolling and local buckling at the crown crest, and the inward radial movement at the springline crest result in tangential stresses.

Elastic analysis that ignores all nonlinear material effects, but includes the nonlinear contact that develops between the pipe and loading platens has the same global horizontal and vertical deflection demands, and similar peak strain demands (Table 2). Thus, material properties have a surprisingly limited effect on the strain demands at any given vertical deflection. Insofar as failure is limited by strain, the deflection at which a parallel plate test will reach peak load may be successfully examined by elastic analysis – ignoring the viscoelastic-plastic nature of the material – but including the nonlinear contact and buckling. This simplification was used in the subsequent analyses reported here.

Table 2 Circumferential stress and strain demands in 1500 mm (60 in.) diameter pipe at 25% deflection predicted from finite element analyses

	Circumferential strain (%)		Circumferential stress MPa (psi)	
	compression	tension	compression	tension
	ϵ_{\min}	ϵ_{\max}	σ_{\min}	σ_{\max}
2.0 in./min	-6.2	4.4	-24.31 (-3,528)	23.40 (3,396)
0.5 in./min	-6.3	4.5	-22.29 (-3,235)	20.88 (3,030)
0.1 in./min	-6.3	4.4	-19.57 (-2,840)	17.53 (2,544)
ELASTIC (1)	-5.2	3.8	-75.79 (-11,000)	62.00 (9,000)

1. Elastic finite element solution includes geometric nonlinearity (as more of the pipe comes in contact with the loading platens and the thin elements buckle) but ignores material nonlinearity.

SIMULATIONS ON SMALLER DIAMETER PIPE

Role of Elastic Modulus

Analysis of 1500 mm (60 in.) diameter pipe shows that the relative performance of different profiles in the parallel plate test may be examined by analysis that considers non-linear geometry, but assumes the material performance is linear elastic. This method is feasible since the strain demands in the parallel plate test are largely a function of the pipe geometry and the contact between the pipe and the plate head, but remain relatively independent of the material elastic modulus. The strain at which buckling occurs is also relatively independent of the modulus. Thus, the primary demand and capacity quantities are dependent on the amount of deformation, and on the geometry, but not the material elastic modulus. The parallel plate test, even with nonlinear geometric effects, is a deformation controlled test. Consider the following numerical example: analysis in the parallel plate test is performed with $E = 108 \text{ MPa}$ (15,710 psi), i.e., one-tenth of the initial modulus. The strain demands in this analysis are identical to the analysis with the initial modulus. In the analysis of the 1500 mm (60 in.) diameter pipe presented previously not all strain demands are recoverable (reversible) and thus the nonlinear viscoelastic-plastic model has slightly higher demands – but for any deformation where the strains are fully recoverable (elastic or nonlinear elastic) the demands are the same. The forces and moments do scale with E , but at a given deflection, the strain demands are unchanged. This fact is further illustrated in Figure 7(a) which shows absolute crown moment vs. deflection and Figure 7(b)

which shows the normalized crown moment (moment divided by peak moment) vs. deflection. The perfect match for the normalized curves shows that strain (i.e., deflections) is independent of modulus.

The capacity in local buckling is also independent of the material modulus. Consider the local buckling strain of a segment of the pipe (for instance the crest) of width, b , thickness, t , and edge restraint defined by k . The elastic buckling strain is

$$\varepsilon_{cr} \propto k \left(\frac{t}{b} \right)^2.$$

Since demand and capacity are independent of the material modulus, use of non-linear geometry, but linear elastic material provides a reasonable method for comparison.

Imperfection Sensitivity

The deflection at peak load, which is important for reliably insuring the 20% deflection limit in the parallel plate test is met, exhibits scatter. This scatter reflects inherent variability in the manufacturing process, but also unavoidable imperfection sensitivity in the buckling response at peak load.

Sensitivity to deflection at peak load was investigated with a finite element model of the parallel plate test. Using the simplified model discussed in the previous section: material elastic, but nonlinear contact and buckling included (geometric nonlinearity), analysis was performed on an 450 mm (18 in.) diameter corrugated plastic pipe. The analysis with no imperfections (i.e., the “ideal” case) results in buckling near the crown at 28% deflection. An analysis with an imperfection with a maximum magnitude of 0.2 mm (0.008 in.), or 10% of the thickness of the crest element ($0.1t_{crest}$), buckling occurs at 22% deflection, for an imperfection of 1 mm (0.04 in.) or $0.5t_{crest}$, buckling occurs at 19% deflection. Figure 8 summarizes these results in a plot of the moment developed at the crown as a function of deflection.

The imperfections used are in the form of small waves near the crown (Figure 9(a) and (b)). The imperfections are superposed and scaled, and used as the initial geometry of the pipe. The small waves are actually the local buckling modes of the pipe under a uniform vertical load over the first twenty degrees. Sensitivity of the failure (i.e., 28% to 19% deflection) to imperfections is not uncommon for buckling phenomena, and combined with other factors, contributes to the scatter observed in experimental results from parallel plate tests. Figure 9(c) and (d) shows that the failure can also be affected by the imperfection.

An assessment of expected imperfection magnitudes can help determine the extent to which imperfection sensitivity is influencing experimental results. However, given the unavoidable thickness variations that occur in the pipe cross-section, around the pipe and along the length, imperfections of such small magnitude are likely to exist regardless. Imperfection sensitivity of this kind is typical for stability critical, thin-walled structures. Based on test results, the imperfection size can be set to reflect the actual variability that is observed.

Strain Demands and Redistribution

For a 450 mm(18 in.) diameter pipe with the $0.5 t_{crest}$ imperfection, the circumferential strain demands developed at the crown of the pipe, as predicted in the finite element analysis, are shown in Figure 10. At approximately 8% deflection the center of the crest buckles and does not carry strains greater than 3.3%. This strain is shed to the corners and at 14% deflection the first portion of the corner peaks at 5.2% strain. The strain continues to increase in the corners until the entire corner buckles and collapse at the crown occurs at 19% deflection and 8% strain. The redistribution of the strain is classic buckling behavior. Observation of this behavior formed the basis for “effective width” ideas suggested by von Kármán, and modified by Winter for use in cold-formed steel design, and recently adopted by AASHTO for incorporating local buckling into the design of profile-wall thermoplastic pipe (5).

Applied vs. Local Strain Demands

We have employed the average strain in the corner as the measure of strain demand (e.g., in Table 2). This strain demand is preferred because it measures the peak average response of the material to the applied deformation, and still accounts for redistribution. Additional measures of the strain demand and the behavior of the strain in pipe with and without small stiffeners in the crest are discussed further here. In the finite element analysis, the strain demand is determined for every element and at five locations through the thickness of each element. Thus, when the question

is asked – at what strain did the pipe fail? – the answer is complicated by the large number of different strains experienced by the pipe. At the crest of the profile, at the crown in the parallel plate test, three measures of strain demand are highlighted in Figure 11.

Strain demand (1) is the peak strain experienced by the pipe. It is the most local measure of the demand and reflects any bending that occurs through the thickness as well as redistribution to the corners. Strain demand (1) is the highest of the three demands, but is localized and “yielding” of the material due to this strain demand does not equate to loss of strength in the corner since the “yielding” to cause failure must occur through the entire thickness, not just at the face.

Strain demand (2) is the average strain in the corner region, and reflects strain redistribution from the web and crest to the corners, but does not reflect local bending. Strain demand (2) is generally considered in the design of thin-walled members that undergo strain redistribution (e.g. cold-formed steel members), since when the average strain is high enough to cause “yielding” the ability of the corner to take greater loads due to further redistribution is compromised. Strain demand (2) is the suggested demand for comparing against material criteria (i.e., yielding).

Strain demand (3) is the strain on the crest as calculated using beam theory, it is the most smoothed (or averaged) measure of the three strain demands. Variation through the thickness and redistribution to the corners is ignored. Strain demand (3) relates to the average *applied* flexural strain, rather than the *material response* measured in strain demands (1) and (2). Existing design calculations essentially consider strain demand (3) as the demand strain.

Strain Demand With and Without a Stiffener

Figure 10 and Figure 12 show the average strain in the corner (strain demand 2) and the strain demand via beam theory (strain demand 3) for a 450 mm (18 in.) diameter pipe with and without a small longitudinal crest stiffener. For pipe where no crest stiffener is present (Figure 10) a large amount of strain redistribution occurs. Thus, the strain demand predicted by beam theory (My/EI) is less than the average strain demand in the corners. Note, in Figure 10 the strain demands agree until the first redistribution occurs (i.e., buckling initiates). When a stiffener is in place (Figure 12) little redistribution of strain occurs, in this case, the average strain in the corner and the beam theory strain demands are essentially the same until the profile buckles.

HAND METHODS

The recently adopted AASHTO design method (6) for profile wall thermoplastic pipe provides methods for calculating pipe capacity in local buckling. At the crown of a parallel plate test the local buckling capacity of a pipe dominates the behavior. However, the local buckling that occurs in a parallel plate test is partially restricted by the steel loading platens and one is left to wonder which scenario is more relevant for the buried pipe: the AASHTO design method which ignores any soil support in local buckling, or the parallel plate test which provides complete support to the crest? While recent work on buried pipe (7) provides insight, classic plate theory provides additional help.

The local buckling strain for a portion of the pipe using small deflection plate buckling equations and ignoring any soil support may be expressed as:

$$\epsilon_{cr} \propto k \left(\frac{t}{w} \right)^2$$

where:

t = thickness

w = width of the plate (e.g. the width of the liner)

k = plate buckling coefficient (e.g. $k=4$ is used for a stiffened element under compression)

Shahwan and Wass (8) investigated local buckling of plates supported by a foundation on one side only. If the support is infinitely stiff, then the plate buckling coefficient (k) is 5.33. Given that the maximum buckling strain increase even for a perfectly rigid foundation is limited to 33%, it seems prudent for general hand methods to ignore this effect. Better soil envelopes around the pipe limit the strain demands, but are limited in their ability to boost the local buckling strain capacity.

The newly adopted design methods also use a flat plate solution for determination of the buckling of an element. It is known that the curvature of the pipe has influence on the solution. Finite element analysis on buckling of curved simply supported plates suggest the following approximate (empirical) solution can be used to account for the increase in the local buckling stress

$$k = 4 + \frac{0.3079(w/t)}{(r/w)}$$

where:

r = radius to the element under consideration, and other variables are previously defined

This expression indicates that tightly curved, stocky elements will see the biggest increase in the elastic buckling strain. For profiles in typical use at the time of this study (diameters from 450 mm to 1500 mm, 15 in. to 60 in.) the average k would be 4.4, an increase of 10% in the elastic buckling strain.

CONCLUSIONS

The material behavior of HDPE is nonlinear viscoelastic-plastic and differs in creep and relaxation. A nonlinear viscoelastic-plastic material model combined with a three-dimensional finite element model of a 90° arc of a single corrugation is capable of predicting the stiffness at 5% and the ultimate behavior of 1500 mm (60 in.) diameter profile wall (corrugated) plastic pipe in a parallel plate test. Additionally, simpler finite element models with elastic material models, but still including all relevant geometric nonlinearity (contact and buckling) can predict the ultimate strain demands and capacity (buckling) in deformation controlled tests such as the parallel plate test. The amount of deflection in the parallel plate test at peak load is unavoidably imperfection sensitive, and scatter should be expected in typical results, even for fine manufacturing tolerances. Local strain demands in the pipe profile can greatly exceed the simple applied strain demands generally assumed in design, due primarily to the out-of-plane bending and redistribution after buckling that occurs as the pipe profile deforms. Hand methods for local buckling predictions which ignore soil support are no more than 33% conservative compared against the ideal support of a parallel plate test. Further ignoring curvature in plate buckling hand methods is on average 10% conservative (for typical corrugated plastic pipe).

ACKNOWLEDGEMENTS

The authors would like to gratefully acknowledge the financial support of Hancor, Inc. in developing the work presented herein. In addition, Lucy Fougner, formerly of Simpson Gumpertz & Heger, Inc. aided in the calculations for the parallel plate analysis of smaller diameter pipe.

REFERENCES

1. Moore, I.D., Zhang, C. (1998). "Nonlinear Predictions for HDPE Pipe Response Under Parallel Plate Loading," *ASC. Journal of Transportation Engineering*, 124 (3) 286-292
2. McGrath, T.J., Schafer, B.W, Moore, I.D., Lesser, A.J. "Thermoplastic Drainage Pipe Design and Testing, Phase 1 Interim Report." NCHRP 4-26. Attachment D, Page D.28, Figure D.21
3. MSC.NASTRAN, www.mscsoftware.com
4. Zhang, C., Moore, I.D. (1997). "Nonlinear Mechanical Response of High Density Polyethylene. Part I: Experimental Investigation and Model Evaluation." *Polymer Engineering and Science*, 37 (2) 404-413
5. McGrath, T.J., Sagan, V.E. (2000). "LRFD Specifications for Plastic Pipe and Culverts." Transportation Research Board, *National Cooperative Highway Research Program (NCHRP)*. Report 438.
6. AASHTO (1998) AASHTO LRFD Bridge Design Specifications, 2nd Edition with 2001 Interim Specifications
7. Schafer, B.W., McGrath, T.J. (2003). "Buried Corrugated Thermoplastic Pipe: Simulation and Design" 2003 Transportation Research Board Annual Meeting, Washington D.C.
8. Shahwan, K.W., Wass, A.M. "Buckling of Unilaterally Constrained Infinite Plates," *ASCE Journal of Engineering Mechanics*, 124 (2) 127-136

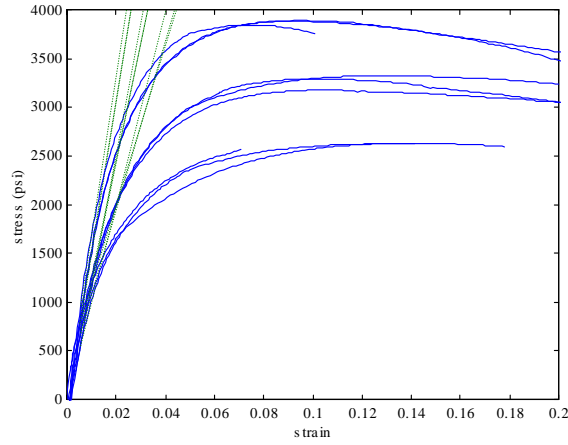


Figure 1 Constant Displacement Rate Test Results: upper three curves tested at 25 mm (1.0 in.)/min., middle three curves tested at 2.5 mm (0.1 in.)/min, final three curves tested at 0.25 mm (0.01 in.)/min.

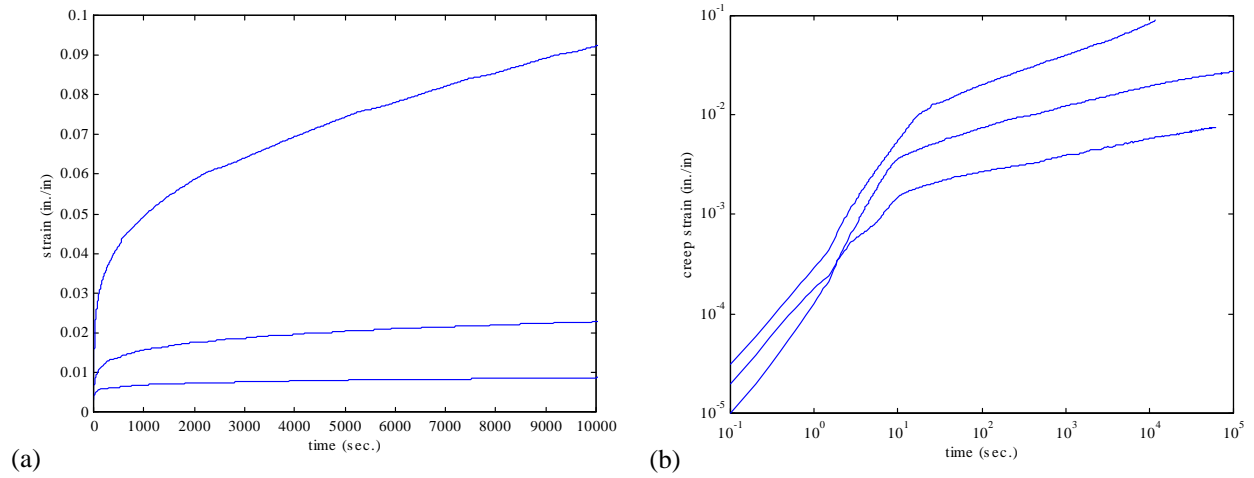


Figure 2 Creep tests results in (a) total strain and (b) creep strain for 13.7 MPa (1982 psi), top curve, 7.5 MPa (1089 psi) and 3.1 MPa (451 psi)

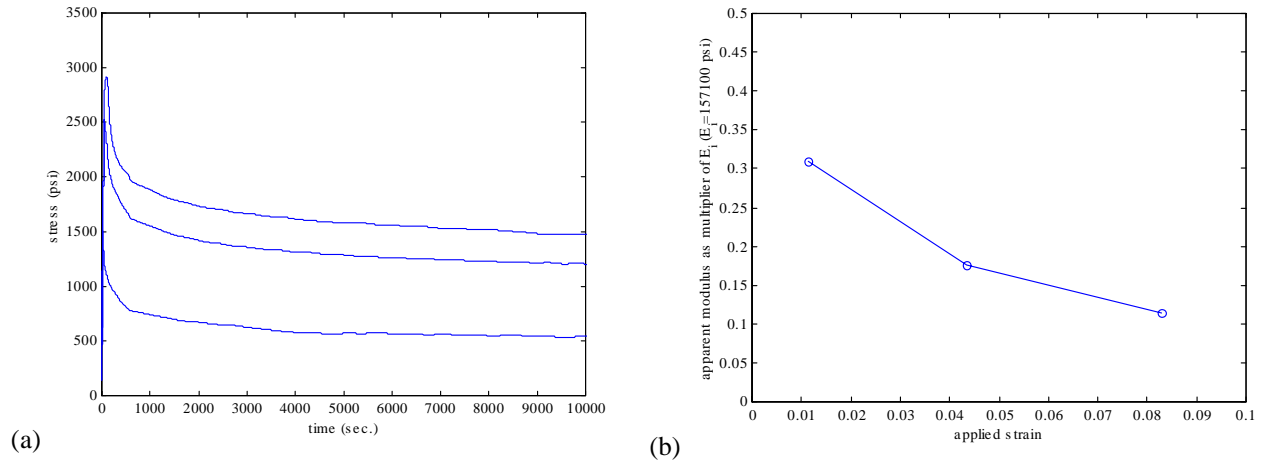


Figure 3 Relaxation test results for 8.3% (upper curve), 4.3% and 1.1% strain (a) and apparent modulus at 10,000 s (b)

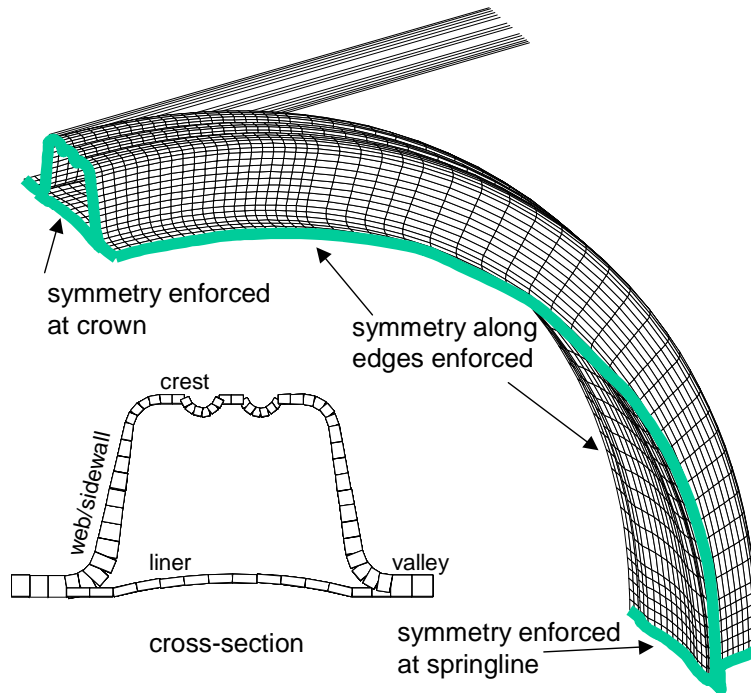


Figure 4 Finite element model for simulation of 90° segment of 1500 mm (60 in.) diameter corrugated plastic pipe

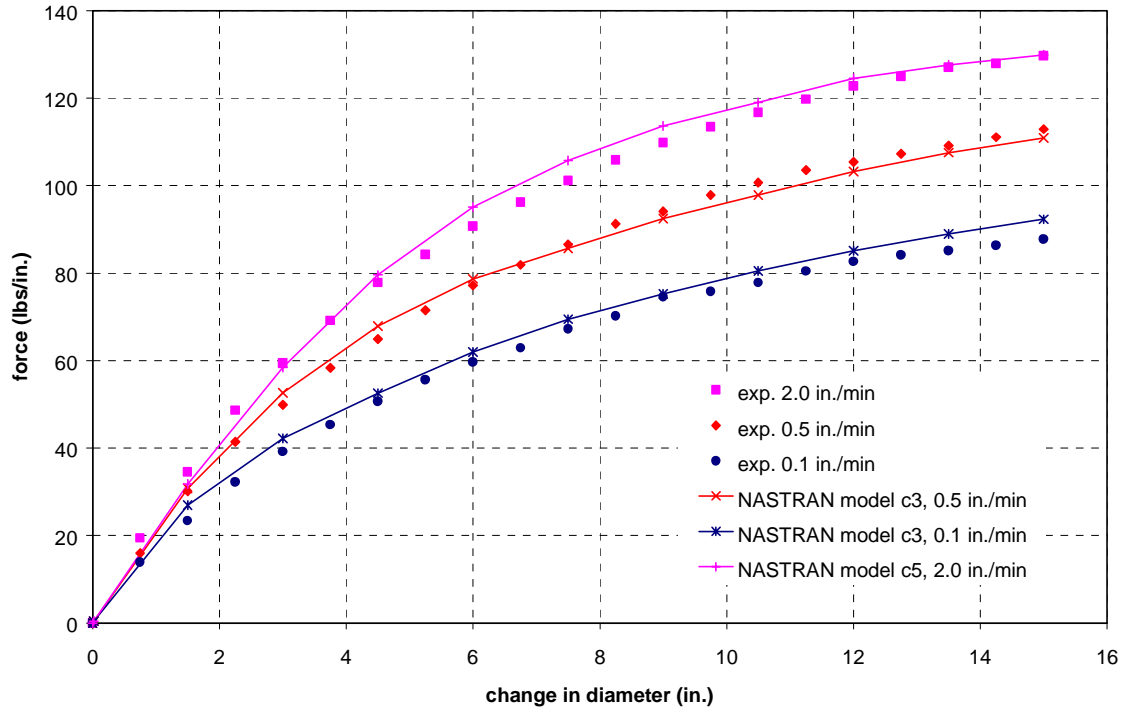


Figure 5 Force vs. vertical diameter change in parallel plate tests and finite element simulations of 1500 mm (60 in.) diameter corrugated plastic pipe

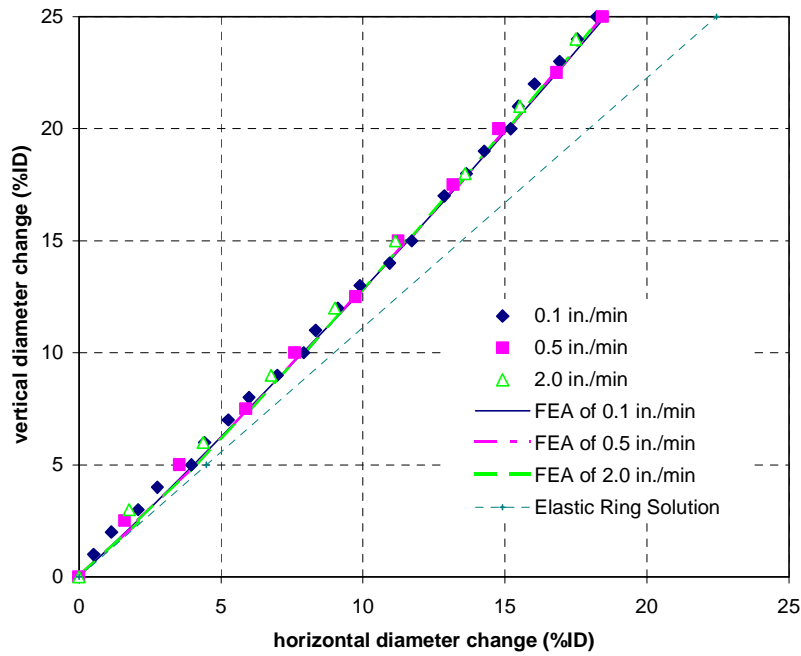
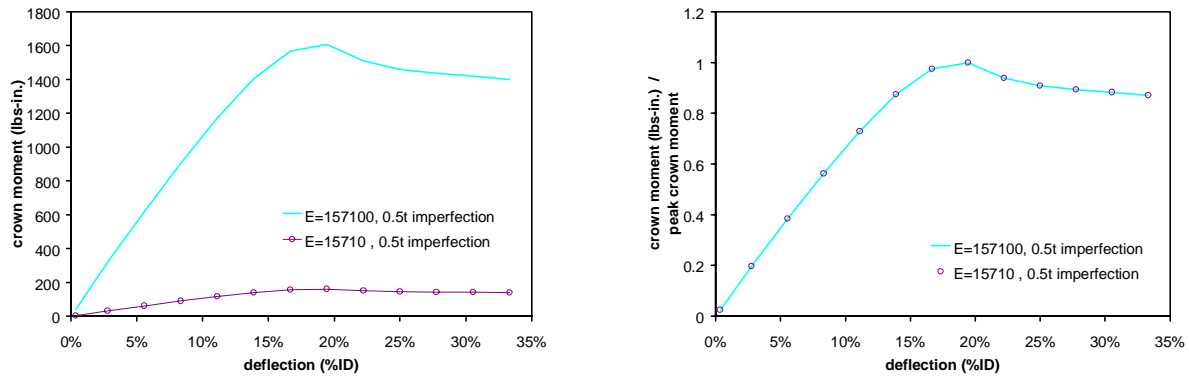


Figure 6 Horizontal vs. vertical diameter change for parallel plate tests and finite element simulation of 1500 mm (60 in.) diameter corrugated plastic pipe



(a) crown moment vs. deflection

(b) normalized crown moment vs. deflection

Figure 7 Role of elastic modulus in the prediction of pipe performance

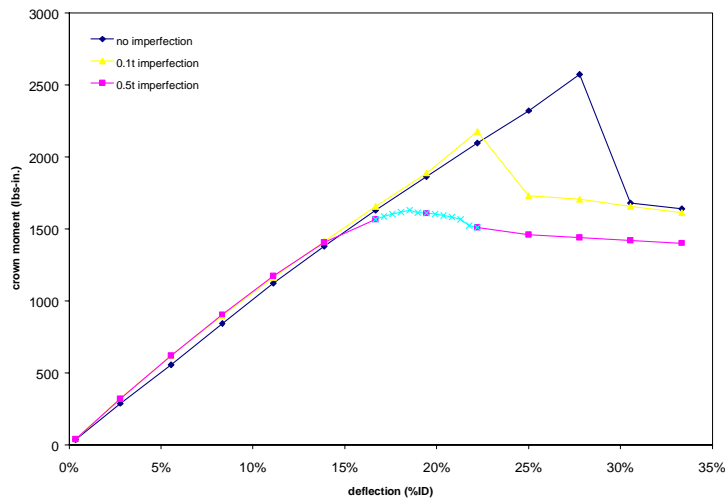


Figure 8 Moment-deflection curve for 450 mm (18 in.) diameter pipe with and without imperfections

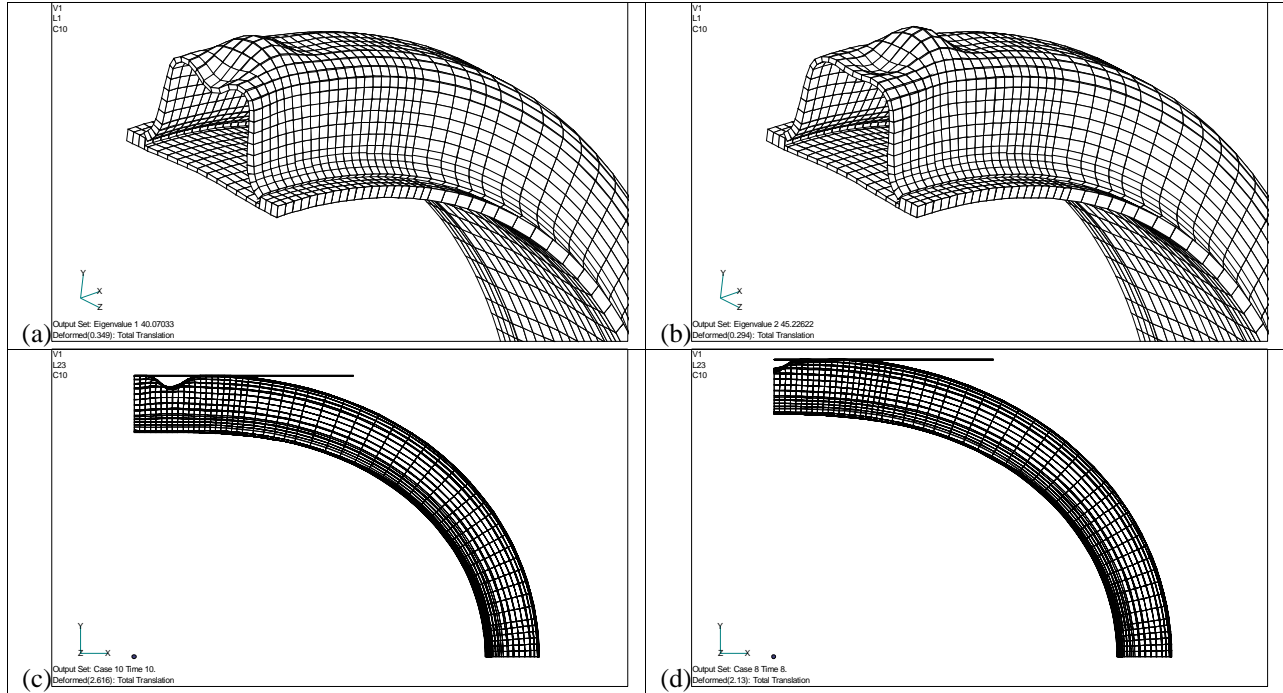


Figure 9 Imperfection shapes (a) and (b) and buckling at 25% deflection for 0.4 mm (0.008 in.) imperfection (c) and 0.2 mm (0.004 in.) imperfection (d) for a 450 mm (18 in.) diameter pipe

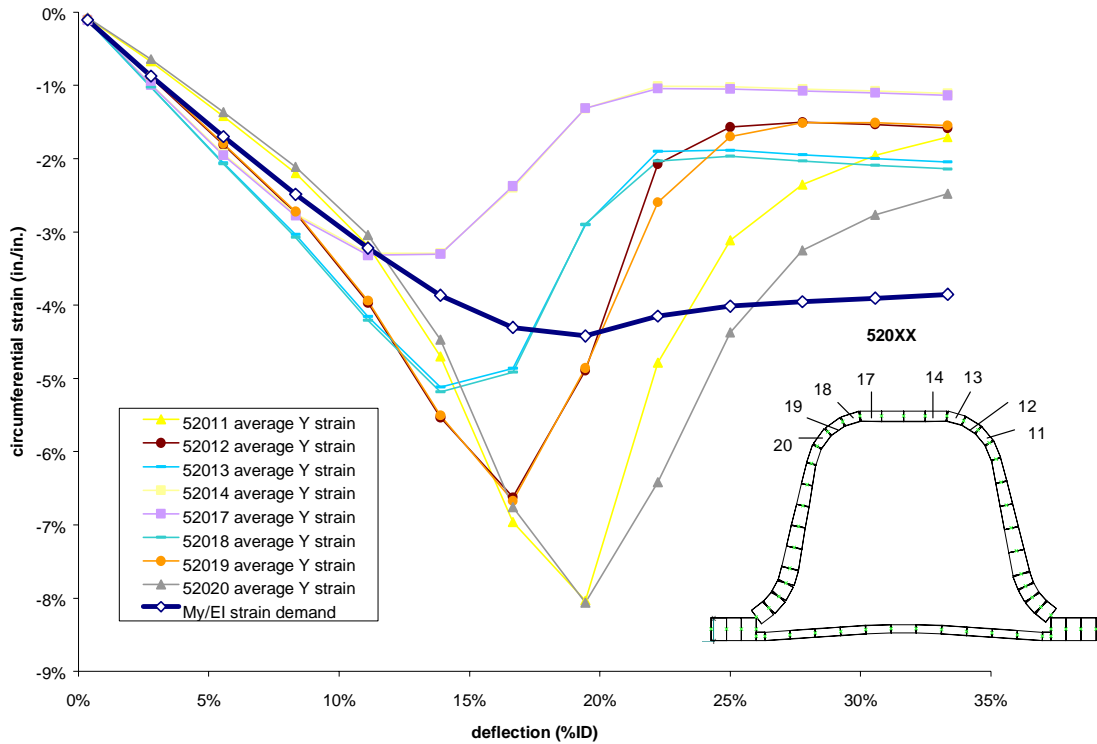


Figure 10 Strain demands at crown in 450 mm (18 in.) diameter pipe

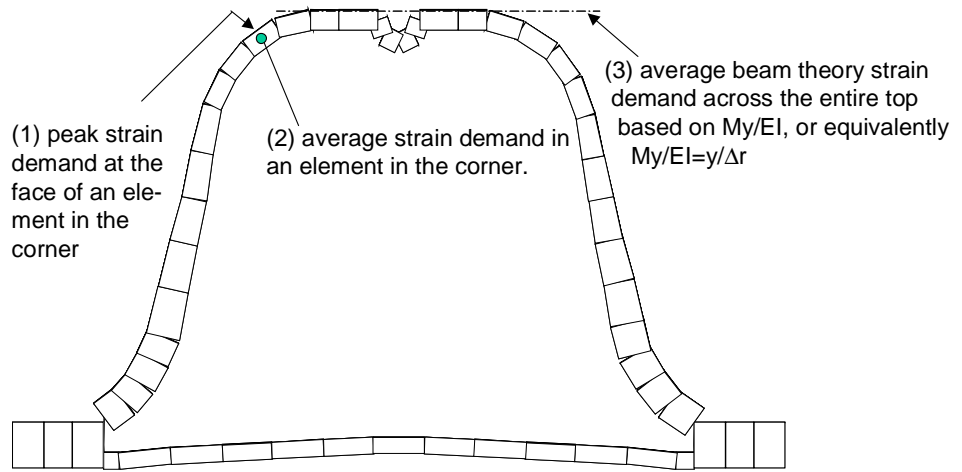


Figure 11 Location and explanation of different strain demands

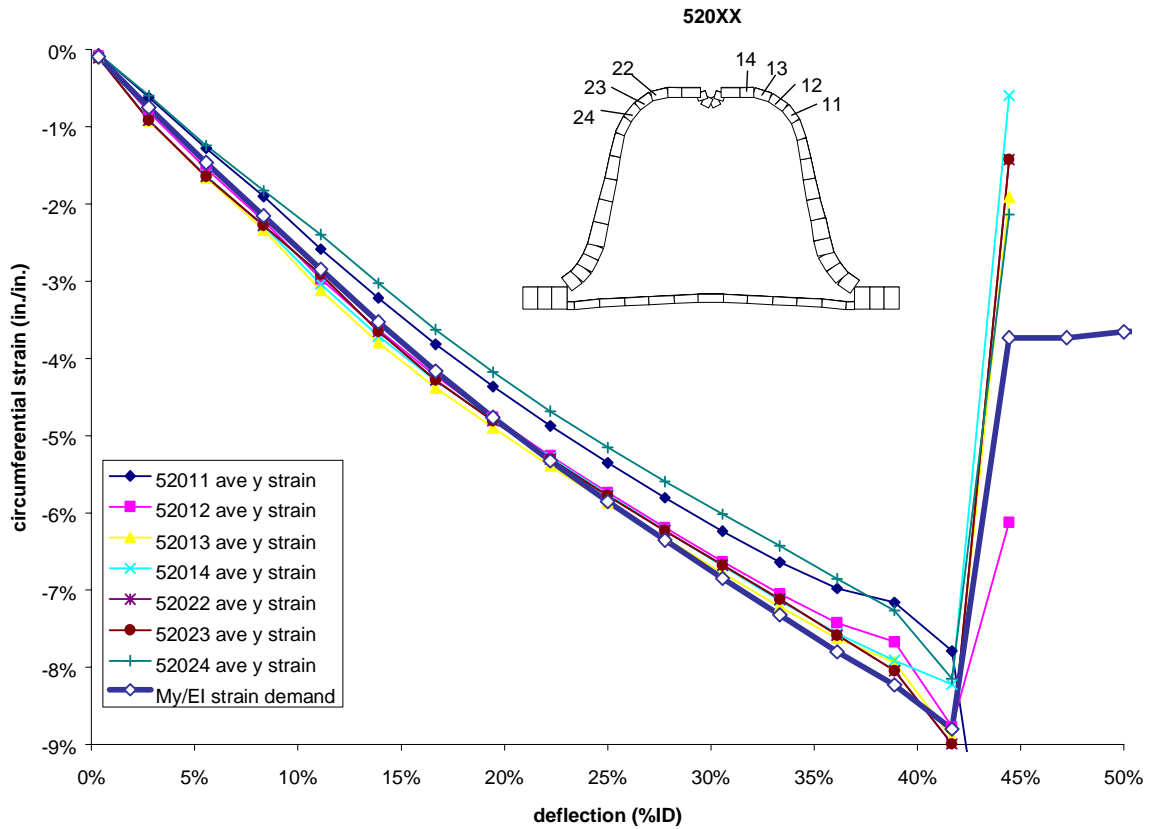


Figure 12 Strain demands in 450 mm (18 in.) diameter pipe with a small crest stiffener